1994 International Conference on Plasma Physics
Foz do Iguaçu - Brazil Contributed Papers 31 Oct. - 4 Nov. 1994

EVOLUTION OF A LOCALIZED LANGMUIR PACKET IN THE SOLAR WIND AND ON AURORAL FIELD LINES

I. Roth, L. Muschietti, E. F. Brown[1]
Space Sciences Laboratory, University of California, Berkeley, CA 94720
P. C. Gray
Bartol Research Institute, University of Delaware, Newark, DE 19716

Langmuir emissions in space are reported to be clumpy and intermittent. The high-frequency wave power appears concentrated in spatial packets, be it amidst the solar wind [1] or on auroral field lines [2]. Due to the plasma motion relative to the spacecraft, determining the source for the wave free energy in the three-dimensional electron distribution function has always been difficult, since the unstable features pass by the detector in presumably too short a time to be measured. The range of unstable phase velocities and growth rates have generally been estimated rather than determined by unequivocal measurements. The analysis of wave-particle interactions in a space environment has taken recently a new turn with the development of wave correlators on board rockets [3] and satellites [4]. Such instruments seek to identify correlations between the phase of the wave-field and the fluxes of energetic particles. The data interpretation is complex, however, and must be backed by a detailed theoretical understanding of the wave-particle interaction, including the phase relation for inhomogeneous packets. To this end Langmuir packets interacting with fast electrons can be studied in the appropriate regime by means of particle-in-cell simulations, provided that one succeeds in reducing the level of the fluctuations, enhancing the signal-to-noise ratio, and incorporating the appropriate boundary conditions. The first results of such simulations are presented here as a test and expansion of previous analysis [5].

The Langmuir packet dimension L is estimated in the solar wind to be of the order of 10-100 km in the direction of the solar wind flow, while on auroral field lines this dimension is of the order of 100-1000 m along the geomagnetic field. Due to the vastly different plasma densities, in both cases the packets contain several tens of wavelengths. When the wave power is concentrated in this manner, the resonant function for the traversing electrons is smooth and the homogeneous wave-train singularity at the phase velocities is removed [5]. The resulting correlation between the phase of the perturbations in the distribution function and the phase of the localized wave determines

(1) The most unstable phase velocities excited by the streaming electrons,
(2) The energy exchange between the waves and the electrons,
(3) The spatial modifications in the downstream non-oscillating distribution function.

The streaming electrons carry with them information about the wave field. The resistive component of the oscillating perturbation is responsible for the energy exchange with the waves, thereby controlling the extent of the packet. When $kL < 4\omega/(k\Delta v_+)$, where Δv_+ is the range of velocities with a positive slope, the ballistic, linear perturbation contains a resistive component which extends the size of the packet downstream. When $kL > 4\omega/(k\Delta v_+)$, the nonlinear component reduces the size of the packet by limiting the range of the energy deposition. Thus there exists a natural packet size which is determined by the velocity range of the positive slope. Availability of a reliable correlator on board satellites can provide an important tool for an analysis of the wave-particle interaction in space, and the numerical as well as analytical understanding of the localized Langmuir packet evolution is of great significance for this purpose.

Following the available experimental data in the solar wind [6] and on auroral field lines, our modelled electrons consist of a bulk distribution, a power-law tail, and a tenuous beam with a positive gradient at large velocities (Figure 1a). This distribution is used in the theoretical analysis as well as in the particle-in-cell simulations. The simulation system resembles the actual physical system by implementing non-periodic boundary conditions, which allows injection of realistic distribution functions at the edges of the simulation box. The system is thus open, with a prescribed flux of particles that enters from one end, interacts self-consistently with the electrostatic field, and leaves at the other end. This scenario resembles the situation of the solar energetic electrons which stream through the solar wind plasma during type III bursts and of the auroral electrons which precipitate into the upper ionosphere after having undergone modulations in the turbulent region at an altitude of 6000 km. Langmuir waves are characterized by a small group velocity; therefore, the resonant electrons cross a packet in a few tens of plasma periods. In the simulation we model the wave-packet by a slowly moving, localized, electrostatic pulse with either a monochromatic structure or with a small random-phase spread about the unstable wave numbers. It

is assumed that the wave was excited locally due to a plasma instability, reaching a weak amplitude of $e\phi/T \lesssim 0.05$, and its finite dimension L parallel to the magnetic field includes tens of wavelengths. We ramp-up an external potential for the first 200 steps (covering a time of $24\omega^{-1}$), allowing the electrons to adjust to the electrostatic field. When the wave reaches the prescribed amplitude, it interacts self-consistently with the plasma.

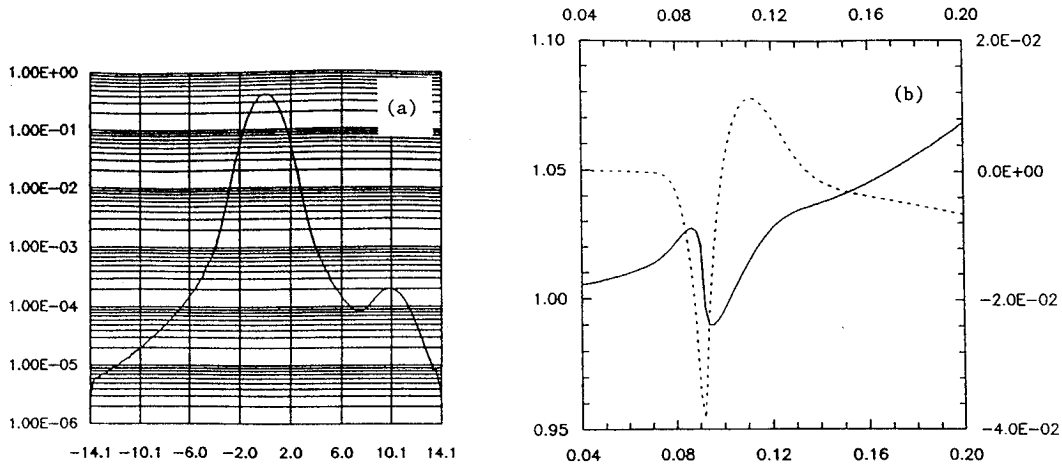

Figure 1. (a) Distribution function described by the core, tail, and beam populations (extended over five orders of magnitude) and used in the simulations. (b) Dispersion relation: $\omega(k)$ - solid curve; $\gamma(k)$ - dashed line. The beam destabilizes a narrow range while the tail damps a broad range of modes.

Figure 1b shows the results of the linear dispersion relation for the complex frequency (normalized to plasma frequency) $\omega = \omega_r + i\gamma$ vs. wavenumber (normalized to the inverse Debye length) for the distribution function of Figure 1a. The core (c) and the beam (b) distributions are given by stationary and the drifting Maxwellians, respectively,

$$F_j(v) = (n_j/(\sqrt{2\pi}u_j))\exp[-0.5[(v - V_j)/u_j]^2] \tag{1}$$

where $j = b, c$, $n_b/n_c = 5 \times 10^{-4}$, $u_b = u_c, V_b = 10u_c, V_c = 0$. The tail (t) distribution is described by

$$F_t(v) = H(v - s)(n_t/(\sqrt{2\pi}u_t))\beta[e^{-\alpha/2}(s/v)^{\alpha} - \exp[-0.5(v/u_t)^2]] \tag{2}$$

where $H(x)$ is the Heaviside function, $\beta = e^{-\alpha/2}\sqrt{\alpha/(2\pi)}/(\alpha - 1) - 0.5[1 - erf(\sqrt{\alpha/2})]$ is the normalization factor, $u_t = u_c, n_t/n_c = 3 \times 10^{-3}$, α is the power-law index, and the junction point with the core distribution functions is given by $s = u\alpha^{1/2}$. This choice satisfies the highest possible degree of analyticity where the combined distribution $F_c + F_t + F_b$ and its first derivative are continuous at $v = s$. In order to evaluate the susceptibility of the tail, we perform a numerical integration over the relevant region in velocity space. To ensure the causality of the Vlasov equation, we follow the general procedure of a Landau contour [7] by adding the contribution of the deformed contour around the pole for $\gamma < 0$. The susceptibilities of the core and of the beam distributions are performed analytically using the standard plasma Z functions for the stationary and the drifting Maxwellians, respectively.

Figure 1b shows that the tail electrons damp the waves except for a narrow range of phase velocities below $\omega/k \approx V_b$. The existence of a tail will confine the unstable spectrum to a narrow range unlike other simulations of beam-plasma instability [8]. Around the resonant phase velocities a deformation of the dispersion relation occurs in both real and imaginary parts due to the beam. This deformation disappears only for very dilute beams [9]. For our parameters the instability is kinetic and occurs on the Langmuir branch.

In order to simulate a realistic distribution as given by Eq. 1-2, which covers five orders of magnitude in phase-space density, and to resolve the important features at the low-density resonant velocities, we divide the macro-particles which occupy the lower density region of phase space into several sub-particles with smaller mass and charge values. This procedure, which preserves the charge-to-mass ratio and the effective plasma frequency is crucial for meaningful results in our parameter regime. Packet size ($kL \sim 10 - 100$), resolution in k space below the resonant wavenumbers, and a sufficiently large simulation

system to analyze the evolution of the packet boundary impose a requirement on a simulation system of the order of a few thousand Debye length λ_D. Sufficient statistics of particles in all regions of phase space at the Debye scale-length and reasonably low noise level ($e\phi/T < 0.05$) require the total number of particles to be greater than one million.

It has been shown previously [5] that in the linear approximation, for a Gaussian electric field envelope $E = E_o \exp[-(x/2L)^2]$, the perturbed distribution is given by

$$f_L(x,v,t) = \frac{eE_0}{m} e^{-\chi^2} e^{i(kx-\omega t)} \frac{\partial F_0}{\partial v} \frac{L}{v}(-i) Z(-\sigma,-\chi) + cc \tag{3}$$

where the real argument of the Z function $\sigma = kL(1 - v_p/v)$ describes the proximity to the phase velocity v_p of the resonant electrons during their traversal through the packet and the imaginary argument of the Z function $\chi = x/2L$ describes the proximity of the measured distribution from the center of the packet. The notable property of the Z function across the real axis gives the asymmetry of the downstream vs. upstream distribution. The function f_L retains the information of the relative phase and also carries its information ballistically to a region outside of the packet. The real part of the complex Z function contributes to the reactive part of the perturbed distribution function and affects mainly the group velocity of the waves. The imaginary part of the complex Z function contributes to the resistive part of the distribution function, which affects the energy exchange between the particles and the wave and causes changes in the wave profile. Similarly, the time-independent distribution function which results from the deformation of the impinging fluxes along their trajectories is given by

$$G(x,v) = \left(\frac{eE_0}{m}\right)^2 \pi \frac{L^2}{v^4} M(v)[e^{-2\sigma^2}(1 + erf(\chi + i\sigma))(1 + erf(\chi - i\sigma))] \tag{4}$$

where $M(v) \equiv kLv_p \frac{\partial F_0}{\partial v} \frac{\partial}{\partial \sigma} - v \frac{\partial F_0}{\partial v} + v^2 \frac{\partial^2 F_0}{\partial v^2}$ and $\mu = (2ekE_o/m\omega^2)(kL)^2$ is the iterative expansion parameter. The nonlinear correction which retains the phase information and takes into account the spatial deformation of the stationary distribution as well as higher-order coupling of the linear perturbation is given by

$$g(x,v,t) = \frac{\mu^3}{(kL)^2} e^{i(kx-\omega t)} \frac{v_p^2}{v} \int_{-\infty}^{\chi} dy\, e^{-3y^2} e^{2i\sigma(y-\chi)} \frac{\partial}{\partial v} \left[\left(\frac{v_p}{v}\right)^4 (P(y,v) + \tfrac{1}{2} Q(y,v))\right] + cc \tag{5}$$

where $P(\chi,v) = v_p \frac{\partial F_0}{\partial v} \left[Z_r(\nu) - \sigma \mid Z(\nu) \mid^2\right] - \frac{v}{4kL} \left(\frac{\partial F_0}{\partial v} - v \frac{\partial^2 F_0}{\partial v^2}\right) \mid Z(\nu) \mid^2$ and
$Q(\chi,v) = v_p \frac{\partial F_0}{\partial v} \left[Z(\nu) - \sqrt{2} Z(\sqrt{2}\nu)\right] + \frac{v}{4kL} \left(\frac{\partial F_0}{\partial v} - v \frac{\partial^2 F_0}{\partial v^2}\right) Z^2(\nu)$ for $\nu = -\sigma - i\chi$.

The resistive part of the linear perturbation f_L and the nonlinear perturbation g constitute the source of the energy exchange between the waves and the particles. For $\mu > 0.6$ the contribution of the nonlinear perturbation becomes comparable to that of the linear perturbation. Figure 2 shows the calculated contribution of the perturbed current and the energy deposition to the packet due to both of the terms. The spatial profile of the linear contribution approximately follows the shape of the packet, resulting in a self-similar growth of the field profile. On the other hand, the non-linear contribution has an opposite sign and its profile is shifted downstream relative to the packet position. The combined contribution is therefore asymmetric with respect to the wave profile, enhancing its amplitude upstream and shrinking its size downstream.

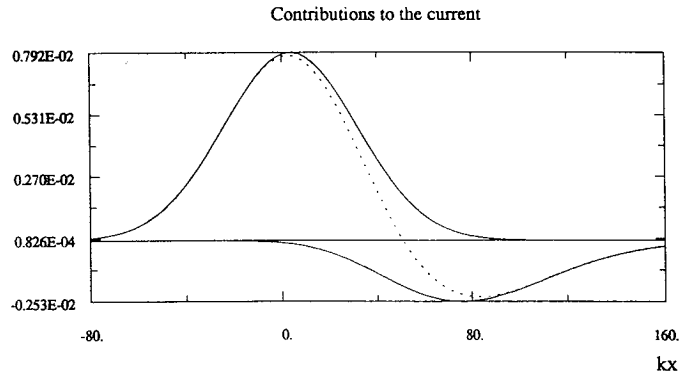

Figure 2. Contributions of the linear (upper solid line), the nonlinear (lower solid line), and the total (dashed line) current, (in arbitrary units) to the energy deposition, as a function of the spatial coordinate. The total contribution indicates a localization of the packet.

Figure 3 shows several snapshots of the wave profile as recorded from a simulation run. The original size of the packet is $kL = 25$; it is ramped-up adiabatically for the time period of $24\omega^{-1}$, and afterwards the packet evolves self-consistently. For low values of $\mu < 1$, the electrons are perturbed according to Eq 4; they exhibit the deformation during the packet traversal and carry the ballistic information downstream. As the packet amplitude is growing, the fresh electrons which enter the system are affected by the stronger electric field. As a result their stationary deformation G increases, and the phase information in the nonlinear perturbed distribution function becomes spatially dependent. The resulting effect on the packet is its growth and localization, as shown at a later time of the simulation.

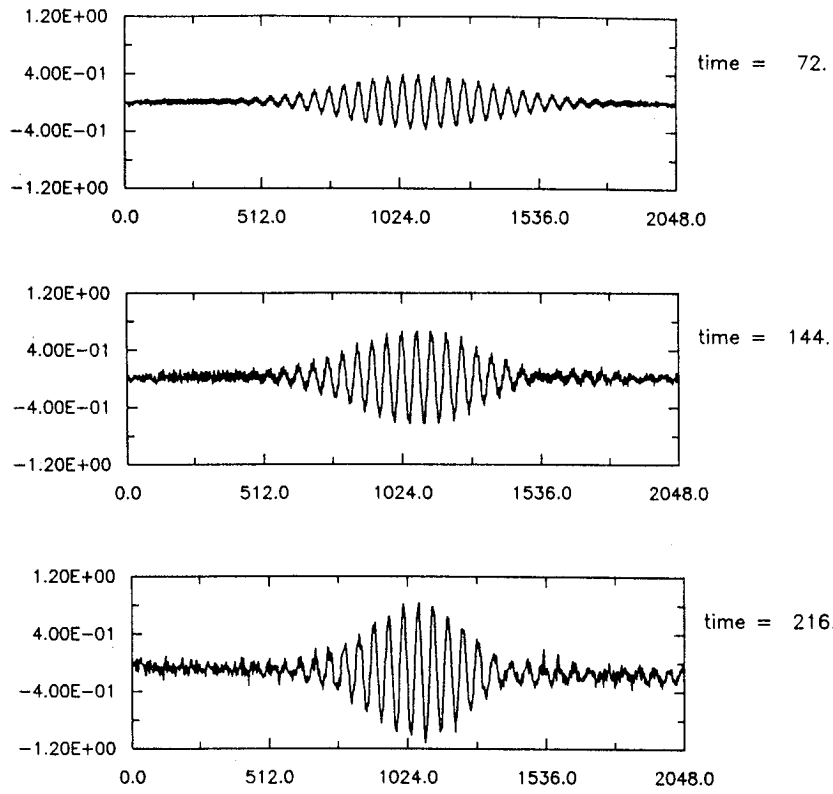

Figure 3. Snapshots of the potential $\Phi(x)$ in units of eT as a function of x (in units of λ_D), recorded at different times of the simulation.

Acknowledgments. This work was supported by NASA grant NAGW-3978.

[1]Also Physics Department, University of California, Berkeley, CA 94720

References

[1] D. A. Gurnett and R. R. Anderson, J. Geophys. Res. 82, 632, 1977.
[2] J. P. McFadden, C. W. Carlson, M. H. Boehm, J. Geophys. Res. 91, 12079, 1986.
[3] R. E. Ergun et al., J. Geophys. Res. 96, 225, 1991.
[4] R. Lundin, EOS Transactions AGU 74, 274, April 1993.
[5] L. Muschietti, I. Roth, R. Ergun, Phys. Plasmas 1, 1008, 1994.
[6] R. P. Lin et al., Astrophys. J. 308, 954, 1986.
[7] N. A. Krall and A. W. Trivelpiece, Principles of Plasma Physics, McGraw-Hill, 1973.
[8] C. T. Dum, J. Geophys. Res. 95, 8095, 1990.
[9] L. Muschietti and C. T. Dum, Phys. Fluids B3, 1968, 1991.